

An Efficient Algorithm for the Calculation of Parasitic Coupling Between Lines in MIC's

John M. Dunn, Lincoln Cole Howard, and Kent Larson

Abstract—A new algorithm is developed to calculate parasitic coupling between transmission lines in an efficient manner. The algorithm works by using the currents and voltages on the lines in the absence of parasitics to calculate independent voltage and current sources which then give the approximate coupling strength between the various lines. These sources are easy to place in a CAD circuit program. The algorithm is demonstrated on a double-stub filter structure. The observed splitting of the resonance, for this particular example, is modeled by using dependent sources, as calculated from the independent sources.

I. INTRODUCTION

PARASITIC coupling is becoming more of a concern in microwave integrated circuits (MIC's) as packing densities of components are increased and frequencies are pushed higher. By parasitic coupling, we mean unintended electromagnetic coupling between two components in the circuit. Such coupling can have a deleterious effect on the circuit's performance.

The effects of parasitic coupling are not included in commercially available circuit simulators at this time. These simulators are based on microwave network theory concepts, and they therefore only include the interaction between two circuit elements if it is specified by the designer. For example, two parallel transmission lines are assumed not to be coupled unless the designer explicitly puts a coupled line model into the circuit. The designer is faced with two problems when trying to include parasitic coupling effects in the circuit design. The first issue is how to determine the strength of the coupling between two elements; the second issue is how to incorporate this effect back into the computer-aided design (CAD) software in a reasonable manner.

One approach that has been tried with some success is to numerically calculate the coupling between the two elements. Typically, the designer inputs the geometry of the two elements into one of the commercially available, full-wave, numerical simulators. The designer obtains an S -parameter file for the frequencies of interest, which is then inserted into the

Manuscript received September 18, 1991; revised October 8, 1992. This work was supported by the National Science Foundation under Contract ECS-8910381.

J. M. Dunn and L. C. Howard are with the Department of Electrical and Computer Engineering, University of Colorado, Boulder, CO 80309.

K. Larson is with the Belvoir Research, Development, and Engineering Center, Department of the Army, Fort Belvoir, VA 22060.

IEEE Log Number 9208341.

circuit simulator. The coupling effect between the two elements is then included. These simulators numerically calculate Maxwell's equations. They, therefore, potentially can include all electromagnetic effects. This goal must be tempered by realistic numerical accuracy limitations, and possible system limitations of the specific simulator used. This approach has two major problems. The first is that circuit simulators are computationally very intensive. Typically, these simulators take several minutes of computation time for each frequency point of interest. The designer is therefore discouraged from calculating parasitic coupling in this manner. The second problem is that the designer gets very little intuitive feeling about how important the coupling is to the circuit's performance. This is a problem if one is trying to correct a parasitics problem or determine its origin in the circuit.

In this paper, we develop an algorithm for calculating parasitic coupling between transmission line elements. The main advantages of the algorithm are that it is quick to implement, and can give the designer an intuitive feeling of the levels of coupling to expect. The formulas are approximate, and therefore subject to a number of limitations. First of all, the algorithm is only developed for microstrip transmission lines. It should be possible to extend it to other transmission line structures. The calculation of coupling between structures which are not transmission lines is outside the scope of the algorithm. Second of all, the algorithm assumes that the lines are far enough apart that the coupling is a small effect. Parasitic is considered here to be a perturbation on the circuit's performance. By this, we mean that the currents and charges on the two lines without coupling included can be used as an initial guess for insertion into the algorithm. This is usually the case in realistic examples. If the coupling is so strong that this assumption is not true, the algorithm may behave poorly.

The algorithm is developed in the next section. It is based on transmission line theory and the inclusion of first-order coupling effects. The effect of coupling is included in the CAD program by inserting independent voltage and current sources in the transmission lines. The third section of the paper demonstrates the algorithm on a coupled-stub structure. This example has been discussed a great deal in the literature. It is known to be a good example of parasitic coupling effects [1]. The algorithm gives coupling of the right strength. It does not, however, produce a splitting of the resonance in the circuit. This defect is remedied by showing how dependent sources may be used for this example in place of independent sources.

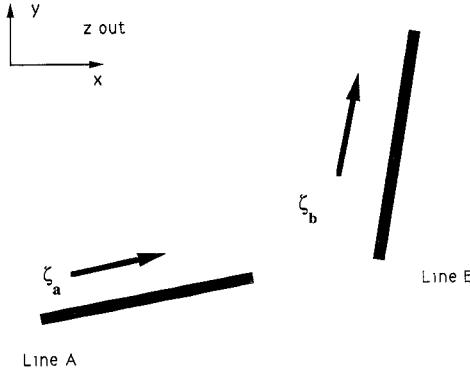


Fig. 1. Lines a and b are coupled by parasitics. The two lines may be oriented at arbitrary angles to one another.

The predicted and experimental results then agree, except for a 150 MHz frequency shift.

II. DERIVATION OF THE ALGORITHM

The algorithm is explained in this section. Assume that we have two transmission lines, labeled a and b . See Fig. 1. The lines may be arbitrarily oriented with respect to one another as long as they lie in the same plane. These lines are usually embedded in an MIC. We wish to calculate the parasitic coupling between lines a and b . Specifically, we wish to find the effect on line b from currents and voltages existing on line a . The entire procedure can later be reversed to calculate the effect on line a from currents and charges on line b . The effect of the coupling will be modeled by placing independent current and voltage sources on line b . The strength of the sources is determined by the current and charge on line a in the absence of coupling. In practice, the CAD program is first run without coupling, and the voltages and currents are found on the lines being examined. The independent voltage and current sources are then calculated and inserted into the circuit. The simulation is then run again.

The voltage and current on the two lines are given by $V_j(\zeta_j), I_j(\zeta_j)$ where $j = a, b$. MKS units are used throughout this paper. The charge/unit length on a line is denoted by $\rho_j(\zeta_j)$. The rectangular coordinate system is defined to have z in the vertical direction. The ground plane is at $z = 0$; the interface between the substrate and air is at $z = h$. The relative dielectric constant of the substrate is denoted by ϵ_r . Only single-layer, nonmagnetic substrates are considered in this paper, although the algorithm could, in principle, be generalized to any transmission line system for which a Green's function exists. Local coordinates along a line are denoted by ζ_a or ζ_b . In actually carrying out the integrals derived in this paper, all local coordinates have to be converted to rectangular coordinates.

We assume that the coupling is weak in the sense that the currents and voltages on the two lines in isolation are not changed dramatically when the coupling is included. It is therefore possible to use the isolated current and voltage on line a as a starting point for calculating the coupling. We also assume that the width of the lines can be neglected. All of the current and charge is lumped into an infinitesimally wide

element. This restriction can be lifted at the cost of increasing the computational time. Assume that charge and current distributions on line a are known in the absence of parasitic coupling. They could be found, in practice, by running the circuit simulator without any parasitics included. The charge and current on the line are the source of electromagnetic fields. These fields excite charges and currents on line b . In reality, there is then an influence back on line a from line b . We ignore this complication because of our assumption of weak coupling. It is more convenient to work with the vector potential A and scalar potential V than with the electromagnetic fields themselves. The voltage and vector potential due to the charges and currents of line a influence line b . The charge and current on line a produce potentials:

$$\begin{aligned} V(x, y) &= \int_{\text{line } a} d\zeta_a \rho_a(\zeta_a) \\ &\quad \cdot ge(\zeta_a; x, y) \\ \vec{A}(x, y) &= \int_{\text{line } a} d\zeta_a \vec{x}_a I_a(\zeta_a) \\ &\quad \cdot gm(\zeta_a; x, y). \end{aligned} \quad (1)$$

The unit vector \vec{x}_a is in the direction of the line a . If the line is not straight, \vec{x}_a changes; this must be included in the integration. The functions ge and gm are Green's functions. They are described in detail in the published literature [2], [3]. The units of ge are 1/farad. The units of gm are henrys/m².

The Telegrapher's equations for line b which include the effect of line a are now derived. Imagine a small length of line b : $\delta\zeta_b$. Faraday's law is applied to this section of line:

$$\oint \vec{E} \cdot d\vec{\zeta}_b = -j\omega \int \vec{B} \cdot d\vec{S}_b. \quad (2)$$

The surface of integration is shown in Fig. 2. The left side of (2) gives the voltage difference between the two ends of the line. The right side of (2) gives magnetic flux going through the surface bounded by the ground plane and transmission line. The source of this flux is due to the current on line b and the incident flux from line a . The current on line b is related to its flux by the transmission line's self-inductance/unit length l_b . Equation (2) thereby becomes

$$\begin{aligned} V_b(\zeta_b + \delta\zeta_b) - V_b(\zeta_b) \\ = -j\omega [l_b I_b(\zeta_b) + A(\zeta_b)] \delta\zeta_b \end{aligned} \quad (3)$$

where A is the component of \vec{A} given by (1), that is, the component in the direction of line b : $A = \vec{A} \cdot \vec{x}_b$. Care must be taken with the signs in (3). The equation can be confirmed by applying Kirchhoff's voltage law to the loop. The self-inductance and the mutual coupling from the other line are voltage drops. This is shown in Fig. 2, where the vector potential A can be envisioned as a voltage source in line b . Taking the limit of line b as $\delta\zeta_b \rightarrow 0$ gives the first Telegrapher's equation:

$$\frac{\partial V_b}{\partial \zeta_b} + j\omega l_b I_b(\zeta_b) = -j\omega A(\zeta_b). \quad (4)$$

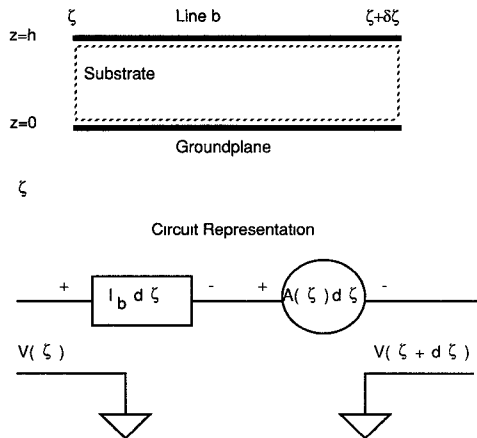


Fig. 2. Surface of integration under line b . The dotted line is the path of the line integral. Also shown is the circuit schematic.

The second of the Telegrapher's equations can be derived by forcing conservation of charge on the second line. The charge and current on line b must obey

$$\frac{\partial I_b}{\partial \zeta_b} + j\omega \rho_b(\zeta_b) = 0. \quad (5)$$

The charge on the line is from two causes. First of all, there is a self-capacitance/unit length on the line: c_b . Since there is a voltage V_b on the line, a charge/unit length

$$\rho = c_b V_b \quad (6)$$

is induced on line b . There is also an electric field near line b from the charge in line a , as given by (1). Because of the mutual capacitance between lines a and b , a voltage difference between the two lines will result in charge being induced on line b . The charge induced must be such to produce a voltage to cancel the electric field from the first line. Otherwise, the voltage given in (6) is not the total voltage on line b . Therefore, there is also an amount of charge/unit length on line b :

$$\rho = -c_b V \quad (7)$$

where V is given by (1). Putting (6) and (7) into (5) gives

$$\frac{\partial I_b}{\partial \zeta_b} + j\omega c_b V_b = j\omega c_b V. \quad (8)$$

This is the second of the Telegrapher's equations.

Equations (4) and (8) must now be solved for I_b and V_b . This is accomplished by standard Green's function methods. The equations are first of all separated:

$$\begin{aligned} \frac{\partial^2 V_b}{\partial \zeta_b^2} - \gamma_b^2 V_b &= -j\omega \frac{\partial A}{\partial \zeta_b} + \omega^2 l_b c_b V \\ \frac{\partial^2 I_b}{\partial \zeta_b^2} - \gamma_b^2 I_b &= j\omega c_b \frac{\partial V}{\partial \zeta_b} - \omega^2 c_b A \end{aligned} \quad (9)$$

where

$$\gamma_b^2 = -\omega^2 l_b c_b. \quad (10)$$

Equations (9) are solved by standard techniques. It is found

$$\begin{aligned} V_b(\zeta) &= \frac{\gamma_b}{2} \int_{\text{line } b} d\zeta_b \left[V(\zeta_b) + \frac{j\omega}{\gamma_b^2} \frac{\partial A}{\partial \zeta_b} \right] \\ &\quad \cdot e^{-\gamma_b |\zeta - \zeta_b|} \\ I_b(\zeta) &= \frac{\gamma_b}{2} \int_{\text{line } b} d\zeta_b \left[-\frac{1}{l_b} A(\zeta_b) + \frac{j}{\omega l_b} \frac{\partial V}{\partial \zeta_b} \right] \\ &\quad \cdot e^{-\gamma_b |\zeta - \zeta_b|}. \end{aligned} \quad (11)$$

The formulas in (11) give the current and voltage on line b due to the currents and charges on line a . In general, there is also a nonzero, homogeneous solution to (9). It is always possible that voltages and currents existed on line b from sources other than line a . The procedure followed here for line a would then have to be repeated for line b . Such charges and currents would be a source of charge and current on line a . In getting (11), it is assumed that each end of line b is terminated in its characteristic impedance. If this is not the case, other waves will exist on the line from reflections off its ends. The effect of these waves will be included when the circuit is resimulated in the CAD program.

Equation (11) is not in a convenient form for insertion into a CAD program. Instead, we now calculate equivalent independent voltage and current sources on line b that give the same response at the ends of the line as that predicted by (11). Once found, the current and voltage sources can be inserted into a CAD program in a straightforward manner. Let the two ends of line b be denoted by ζ_{lo} and ζ_{up} . We now imagine a line with a voltage source in series and a current source in shunt, as shown in Fig. 3. The voltage source has strength V_0 , and is located at a position $\zeta_b = s_V$. The current source is of strength I_0 , and is located at position $\zeta_b = s_I$. To the right of the two sources, $\zeta_b > s_I$ and $\zeta_b > s_V$, only a wave moving to the right exists. Its voltage and current are given by

$$\begin{aligned} V^+(\zeta_b) &= \frac{1}{2} V_0 e^{-\gamma_b (\zeta_b - s_V)} \\ &\quad + \frac{1}{2} Z_c I_0 e^{-\gamma_b (\zeta_b - s_I)} \\ I^+(\zeta_b) &= \frac{1}{2 Z_c} V_0 e^{-\gamma_b (\zeta_b - s_V)} \\ &\quad + \frac{1}{2} I_0 e^{-\gamma_b (\zeta_b - s_I)} \end{aligned} \quad (12)$$

where Z_c is the characteristic impedance of line b . To the left of the sources, $\zeta_b < s_I$ and $\zeta_b < s_V$, there is only a wave going to the left. Its voltage and current are given by

$$\begin{aligned} V^-(\zeta_b) &= \frac{1}{2} V_0 e^{\gamma_b (\zeta_b - s_V)} \\ &\quad + \frac{1}{2} Z_c I_0 e^{\gamma_b (\zeta_b - s_I)} \\ I^-(\zeta_b) &= \frac{1}{2 Z_c} V_0 e^{\gamma_b (\zeta_b - s_V)} \\ &\quad - \frac{1}{2} I_0 e^{\gamma_b (\zeta_b - s_I)}. \end{aligned} \quad (13)$$

The sources V_0 and I_0 are required to give the same voltage and current at the ends of the lines as is predicted by (11). Matching (11) with (12) and (13) at $\zeta_b = \zeta_{lo}$ and $\zeta_b = \zeta_{up}$

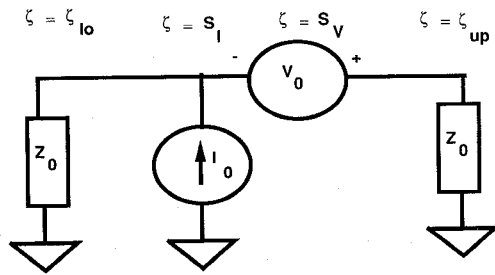


Fig. 3. Transmission line with independent source and independent

gives

$$V_0 = D \int_{\text{line } b} d\zeta_b \{ \gamma_b V(\zeta_b) \cdot \sinh[\gamma_b(\zeta_b - s_I)] - j\omega A(\zeta_b) \cdot \cosh[\gamma_b(\zeta_b - s_I)] \}$$

$$I_0 Z_b = D \int_{\text{line } b} d\zeta_b \{ \gamma_b V(\zeta_b) \cdot \cosh[\gamma_b(\zeta_b - s_V)] - j\omega A(\zeta_b) \cdot \sinh[\gamma_b(\zeta_b - s_V)] \} \quad (14)$$

where

$$D = \frac{1}{\cosh[\gamma_b(s_V - s_I)]}. \quad (15)$$

Z_b is the characteristic impedance of line b . Equation (14) is the final, desired equation.

To summarize, the current and charge on line a are first calculated without parasitic coupling. Equivalent independent voltage and current sources on line b can then be calculated, which approximately give the effect of coupling due to line a . These current and voltage sources can then be inserted into a CAD program if desired.

III. EXAMPLE OF TWO COUPLED STUBS

In this section, the algorithm is applied to a simple stub filter structure. The circuit is shown in Fig. 4. The structure has been studied extensively [1], and is known to be sensitive to parasitic coupling. The circuit was built on alumina substrate, with $\epsilon_r = 9.6$, substrate thickness $h = 125 \mu\text{m}$, and line widths of $122 \mu\text{m}$. This makes the characteristic impedances of all lines close to 50Ω . The stub lengths are 2.921 mm . The separation between the stubs was varied, with experimental values ranging from 0 to $757 \mu\text{m}$. Separation is defined to be the center-to-center distance.

The predicted performance for the circuit agrees with the measured results, except for $|S_{21}|$ near 10 GHz. The separation between the stubs is $757 \mu\text{m}$. The theoretical results were calculated using a commercially available microwave circuit program [4], in which no parasitic coupling between lines was included. The substrate was assumed to be lossless; the lines were made of gold, and were $1.5 \mu\text{m}$ thick. The discrepancy in $|S_{21}|$ near 10 GHz appears as a "double-dip" in the experimental results, but not the simulated. This region is shown in Fig. 5. Such a splitting of a resonance is characteristic

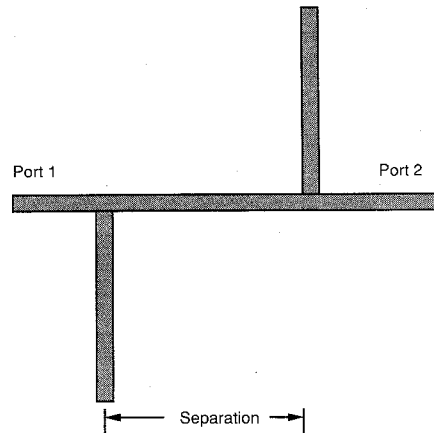
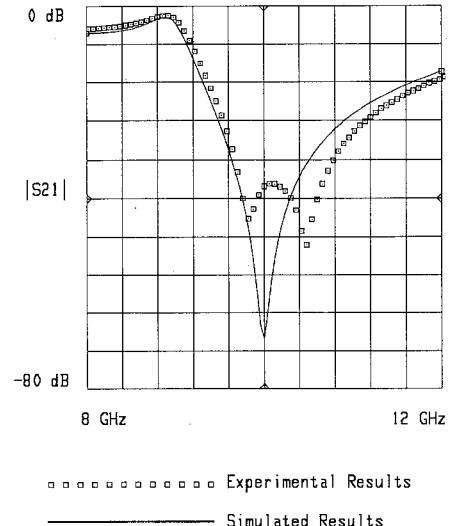


Fig. 4. Double-stub filter structure to be analyzed for parasitics.

Fig. 5. Theoretical values with no coupling versus measured values for $|S_{21}|$. A discrepancy is noted near 10 GHz in $|S_{21}|$.

of coupled resonators. Parasitic coupling between the stubs is therefore suspected.

It is, first of all, necessary to calculate the voltage and current without coupling in order to implement the algorithm described in the previous section. We do so at the resonance of the stubs, where the parasitic coupling is expected to be important. At resonance, the stubs are $1/4$ of a wavelength long; they appear as shorts to the main line. It is therefore assumed that the incident wave from port 1 is entirely reflected back. Furthermore, a current and voltage exist on the left stub. They are given by

$$I(\zeta) = I_m \frac{\sin[\beta_e(\zeta + \zeta_s)]}{\sin[\beta_e \zeta_s]} \quad (16)$$

$$V(\zeta) = V_m \frac{\sin[\beta_e \zeta]}{\sin[\beta_e \zeta_s]}.$$

The wavenumber is β_e . The stub length is ζ_s . The ends of the stub are at $\zeta = 0$ and $\zeta = -\zeta_s$. The maximum current I_m occurs at the beginning of the stub. The maximum voltage V_m occurs at the end of the stub. The current and voltage are not independent, but are related by the Telegrapher's equations

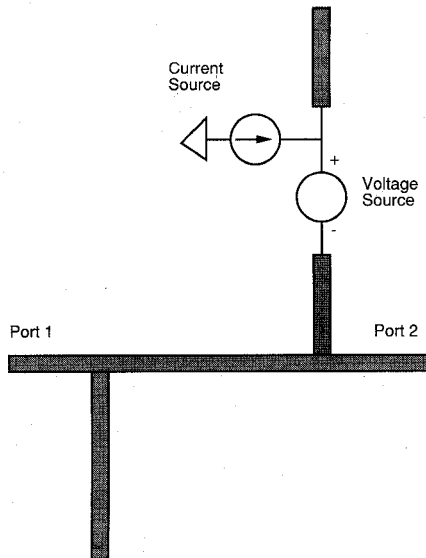


Fig. 6. Schematic of the double-stub structure with independent parasitic sources in the middle of the right stub.

These give

$$V_m = -jZ_c I_m \quad (17)$$

where Z_c is the characteristic impedance of the stub.

It is desired to find the S -parameters for the circuit with independent voltage and current sources placed in the right stub. It first must be decided where the independent sources are to be placed. The choice is somewhat arbitrary. We placed the sources in the middle of the right stub, as shown in Fig. 6. The strengths of the sources are calculated by using (14). The amplitude of the current and voltage in the left stub are determined by assuming 1 W of incident, average power from port 1. This sets $I_m = 2/\sqrt{50}$ and $V_m = -j2\sqrt{50}$ V, where I_m and V_m are the complex amplitude of the current and charge on the left stub, as in (16). The integrals to determine the voltage and current source were numerically evaluated using Simpson's rule in two dimensions. Ten steps in each direction gave accuracy comparable with the approximate Green's functions being used [3], about three digits for the present problem. The current and voltage sources were determined to be $V_0 = 0.00607 + j0.044$ V and $I_0 = -0.000817 + j0.000300$ A.

The S -parameters are found by examining the power coming out of ports 1 and 2. A circulator was inserted at port 1 in order to get isolation between the input and output directions. The magnitude of S_{21} is shown in Fig. 7, where the independent sources have been inserted. Note that the strength of the sources was not varied with frequency. It was felt that this would lead to a very small change in the fixed results. The insertion of the sources have brought the curve up substantially. The designer can see that parasitic coupling is a problem for this circuit. The splitting of the resonance has not, however, been modeled. The reason for this is that it is not possible to change a linear circuit's response by inserting independent sources; only dependent sources can change the nature of the filter's response curve.

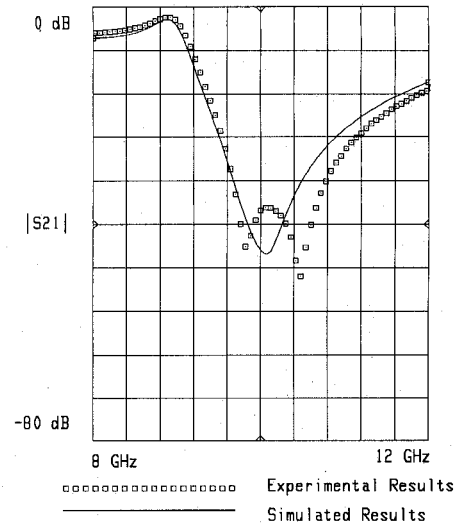


Fig. 7. Independent source results versus experimental points for $|S_{21}|$ near 10 GHz.

The first attempt at remedying this problem was to replace the independent sources by dependent ones. The problem is that there are a number of possible choices for dependent sources, depending on what one wants for the control variable, and where that variable should be measured. For example, should a dependent voltage source be a current- or voltage-controlled source, or perhaps some combination of the two? Different choices lead to different answers. For this particular problem, we found a way to make the method work. It is important that the dependent sources retain the symmetry of the underlying geometry. For example, coupling between the middle of each stub would keep the right symmetry. However, we then do not know if we want current or voltage control. At the ends of the stubs, we know the current is zero. We therefore must have a voltage-controlled source if we couple the ends of the lines. The obvious choice is a capacitor. The beginning of the stubs has almost zero voltage at resonance. We therefore must have current-controlled sources if we couple to the beginning of the stubs. We therefore chose a mutual inductance.

We therefore placed a dependent voltage source at the ends of the stubs, a mutual capacitor; and a dependent current source at the beginning of the stubs, a mutual inductor. We can determine the value of the capacitor and inductor by requiring that the strength of the dependent sources be the same at the independent sources.

Equation (14) must be modified if independent sources are going to be inserted at the beginning and end of the right stub. This is because the parameter D becomes arbitrarily large if the two sources are placed a quarter of a wavelength apart, as is the case for the stubs at resonance. We therefore need to modify (14) for this case. The derivation of the previous section is modified by assuming that line b is open at one end and shorted at the other end. The length of the line is l . A series voltage source is placed at $\zeta = 0$, and a shunt current source is placed at $\zeta = l$. See Fig. 8. Standard transmission line theory

predicts the strength of the voltage and current sources as

$$\begin{aligned} V_0 &= V(\zeta) \cos(\beta\zeta) + jZ_0 \sin(\beta\zeta) \\ I_0 &= -I(\zeta) \cos[\beta(\zeta - l)] \\ &\quad + \frac{j}{Z_0} V(\zeta) \sin[\beta(\zeta - l)] \end{aligned} \quad (18)$$

where $V(\zeta)$ and $I(\zeta)$ are the voltage and current on the line produced by V_0 and I_0 . The voltage and current on the line are in the form of a TEM mode. It is desired to come up with the "best" value of V_0 and I_0 when a wave is incident from the other line. The stub is about a quarter wavelength long. Therefore, if we pick V_0 to give the correct voltage at $\zeta = l$, we should have an accurate solution along the entire stub. Similarly, we require the current source I_0 at the end of the stub to give the correct current at the beginning of the stub, $\zeta = 0$. We therefore require (18) to be true at $\zeta = l$ for the voltage source and $\zeta = 0$ for the current source:

$$\begin{aligned} V_0 &\approx V(l) \cos(\beta l) \\ &\quad + jZ_0 I(l) \sin(\beta l) \\ I_0 &\approx -I(l). \end{aligned} \quad (19)$$

We can neglect the term with $I(l)$ in it for the calculation of V_0 . This is because the current will be much smaller than the voltage at the open end $V(l)$. Then

$$\begin{aligned} V_0 &\approx V(l) \cos(\beta l) \\ I_0 &\approx -I(l). \end{aligned} \quad (20)$$

We still need to find the $V(l)$ and $I(l)$ induced on the stub from the voltage and current on the first stub. Equations (9) are solved for V_b and I_b . Line b is now shorted at $\zeta_b = 0$ and open at $\zeta_b = l$. By using standard techniques, the solution is found to be

$$\begin{aligned} V_b(\zeta_b) &= \int_0^l d\zeta_0 \left[-V(\zeta_0) + \frac{j\omega}{\beta^2} \frac{\partial A}{\partial \zeta_0} \right] \\ &\quad \cdot G_v(\zeta_0; \zeta_b) \\ Z_0 I_b(\zeta_b) &= j \int_0^l d\zeta_0 \left[-V(\zeta_0) + \frac{j\omega}{\beta^2} \frac{\partial A}{\partial \zeta_0} \right] \\ &\quad \cdot G_I(\zeta_0; \zeta_b) \end{aligned} \quad (21)$$

where the Green's functions G_v and G_I are given by

$$\begin{aligned} G_v &= \frac{\beta \cos[\beta(\zeta_0 - l)] \sin(\beta\zeta_b)}{\cos(\beta l)} \\ &\quad 0 < \zeta_b < \zeta_0 \\ &= \frac{\beta \cos[\beta(\zeta_b - l)] \sin(\beta\zeta_0)}{\cos(\beta l)} \\ &\quad \zeta_0 < \zeta_b < l \\ G_I &= \frac{\beta \cos[\beta(\zeta_0 - l)] \cos(\beta\zeta_b)}{\cos(\beta l)} \\ &\quad 0 < \zeta_b < \zeta_0 \\ &= \frac{\beta \sin[\beta(l - \zeta_b)] \sin(\beta\zeta_0)}{\cos(\beta l)} \\ &\quad \zeta_0 < \zeta_b < l. \end{aligned} \quad (22)$$

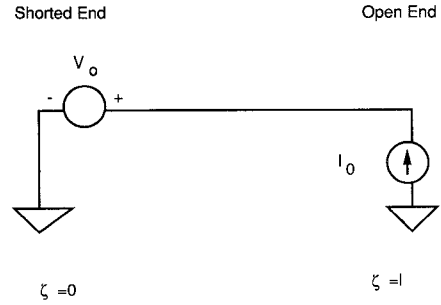


Fig. 8. Current and voltage sources placed at the ends of a line, one end of which is shorted, the other open.

Equations (21) are used to find V_0 and I_0 in (20). The final expressions for the sources are

$$\begin{aligned} V_0 &= \int_0^l d\zeta_0 \left[-\beta V(\zeta_0) \sin(\beta\zeta_0) \right. \\ &\quad \left. - j\omega A(\zeta_0) \cos(\beta\zeta_0) \right] \\ I_0 &= \int_0^l d\zeta_0 \left[\frac{j\beta}{Z_0} V(\zeta_0) \cos[\beta(\zeta_0 - l)] \right. \\ &\quad \left. + \frac{\omega}{Z_0} A(\zeta_0) \sin[\beta(\zeta_0 - l)] \right]. \end{aligned} \quad (23)$$

Finally, we find the mutual capacitance C_m and mutual inductance M by

$$\begin{aligned} M &= \frac{V_0}{j\omega |I_m|} \\ C_m &= \frac{I_0}{j\omega |V_m|}. \end{aligned} \quad (24)$$

It should be noted that complex values of capacitance and inductance will often result from this procedure. This reflects the fact that there is a phase dependence in the Green's functions. Inserting a complex capacitance or inductance can result in a violation of energy conservation. This should not cause concern as the method is approximate and the discrepancy in energy is small. Stated more mathematically, the error in energy is second order in the small expansion parameter of the coupling, and the theory is only accurate to first order in the coupling.

Fig. 9 shows the results of the simulation when the calculated C_m and M are used for a stub separation of 757 μm . The agreement is seen to be good. Values of $C_m = 1.30 \times 10^{-15} - j2.14 \times 10^{-16}$ F and $M = 3.22 \times 10^{-12} - j5.36 \times 10^{-13}$ H were used. (The inductance was given an extra 180° phase shift from the value listed here when inserted into the CAD program. This is because the mutual inductance in the circuit program has a voltage sign convention opposite that given by Faraday's law.) If the simulated results are shifted by 150 MHz, the curves lie on top of one another. The agreement is also good for smaller separations. Fig. 10 shows the case for 249 μm apart, corresponding to a separation of two substrate thicknesses. The calculated values of inductance and capacitance are $C_m = 3.80 \times 10^{-15} - j2.15 \times 10^{-16}$ F and $M = 9.37 \times 10^{-12} - j5.38 \times 10^{-13}$ H. (The actual inductance put in the CAD program was again shifted by 180° to give the correct sign convention for mutual inductance.) The integrals

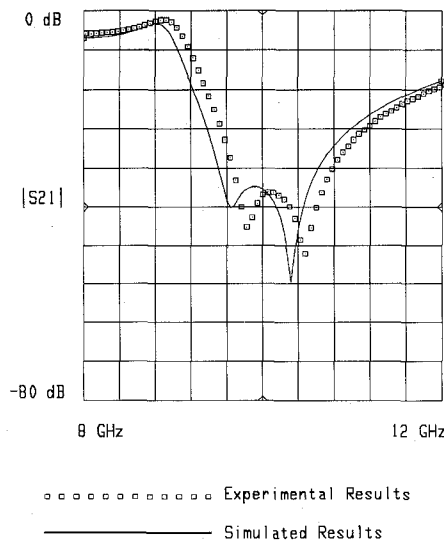


Fig. 9. Comparison of experimental and theoretical values for $|S_{21}|$ with mutual capacitance and inductance included. A separation of $757 \mu\text{m}$ is used.

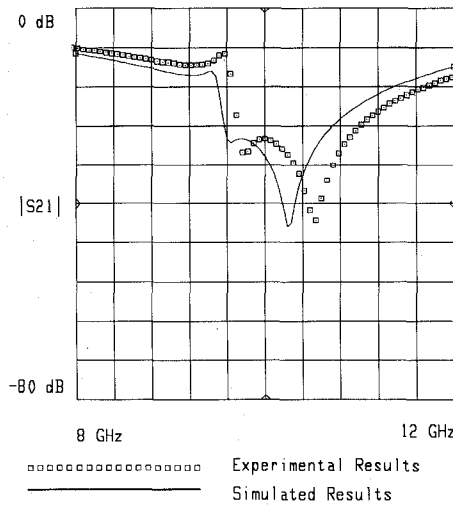


Fig. 10. Comparison of experimental and theoretical values for $|S_{21}|$ with mutual capacitance and inductance included. A separation of $249 \mu\text{m}$ is used.

were calculated using a two-dimensional Simpson's rule. Ten steps in each dimension were found to be adequate to assure convergence.

IV. CONCLUSIONS

A method has been developed to include parasitic coupling effects between transmission lines in MIC's. The method uses the voltages and currents on the lines without coupling to calculate independent voltage and current sources. These sources can then be inserted into the CAD program.

A specific example of a double tee was examined. The algorithm correctly gave the coupling strength. It did not give

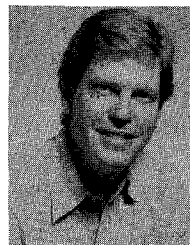
the splitting of the resonance. This was accounted for by modifying the algorithm to calculate dependent sources; in this case, they were mutual inductances and capacitances. The agreement between experimental and simulated results was reasonable.

ACKNOWLEDGMENT

The authors wish to thank J. Neyland and D. Pon for providing them with the experimental data.

REFERENCES

- [1] M. Goldfarb and A. Platzker, "The effects of electromagnetic coupling on MMIC design," *Microwave and Millimeter Wave CAE*, vol. 1, pp. 38-47, Jan. 1991.
- [2] J. Mosig, "Integral equation technique," in *Numerical Techniques for Microwave and Millimeter-Wave Passive Structures*, T. Itoh, Ed. New York: Wiley, 1989, ch. 4.
- [3] J. M. Dunn, "A uniform asymptotic expansion for the Green's functions used in microstrip calculations," *IEEE Trans. Microwave Theory Tech.*, vol. 39, pp. 1223-1126, July 1991.
- [4] Hewlett-Packard Microwave Design System, Hewlett-Packard Co., Santa Rosa, CA.
- [5] K. C. Gupta, R. Garg, and R. Chadha, *Computer-Aided Design of Microwave Circuits*. Dedham, MA: Artech House, 1981.



John M. Dunn was born in St. Paul, MN, on September 22, 1956. He received the B.A. degree in physics from Carlton College, Northfield, MN, in 1978, the S.M. degree in 1980, and the Ph.D. degree from Harvard University, Cambridge, MA, in 1984, both in applied physics.

From 1984 to 1986 he worked at Sandia National Laboratories as a member of the technical staff, responsible for various electromagnetics problems in the areas of EMP and radar. In 1986 he joined the faculty of the Department of Electrical and Computer Engineering, University of Colorado, where he is currently an Associate Professor. His research interests include the modeling of electromagnetic elements, especially for CAD programs, numerical simulation of electromagnetic fields problems, and the development of fast algorithms for microwave CAD programs.



Lincoln Cole Howard was born in Salt Lake City, UT. He received the B.S. degrees in physics and electrical engineering from the Massachusetts Institute of Technology, Cambridge, in 1984.

From June 1984 to August 1989 he worked at M.I.T. Lincoln Laboratory as a Microwave Engineer. He is currently pursuing the Ph.D. degree at the University of Colorado, Boulder.

Kent Larson, photograph and biography not available at the time of publication.